Inorganic Chemistry

Article

pubs.acs.org/IC

New Layered Fluorosulfide $SrFBiS_2$

Hechang Lei, Kefeng Wang, Milinda Abeykoon, Emil S. Bozin, and Cedomir Petrovic*

Condensed Matter Physics and Materials Science Department, Brookhaven National Laboratory, Upton, New York 11973, United States

Supporting Information

ABSTRACT: We have synthesized a new layered BiS_2-based compound, $SrFBiS_2$. This compound has a similar structure to $LaOBiS_2$. It is built up by stacking up SrF layers and NaCl-type BiS_2 layers alternatively along the c axis. Electric transport measurement indicates that $SrFBiS_2$ is a semiconductor. Thermal transport measurement shows that $SrFBiS_2$ has a small thermal conductivity and large Seebeck coefficient. First principle calculations are in agreement with experimental results and show that $SrFBiS_2$ is very similar to $LaOBiS_2$, which becomes a superconductor with F doping. Therefore, $SrFBiS_2$ may be a parent compound of new superconductors.

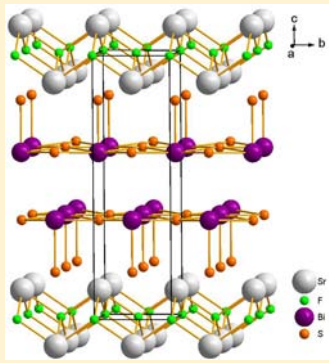

INTRODUCTION

Low-dimensional superconductors with layered structure have been extensively studied and still attract much interest due to their exotic superconducting properties and mechanism when compared to conventional BCS superconductors. The examples include high T_c cuprates,[1] Sr_2RuO_4,[2] $Na_xCoO_2{\cdot}H_2O$,[3] and iron-based superconductors.[4] The discovery of LnOFePn (Ln = rare earth elements, Pn = P, As) in particular revitalizes the study of layered compounds with mixed anions, paving a way to materials with novel physical properties. For example, $Ln_2O_2TM_2OCh_2$ (TM = transition metals, Ch = S, Se) show strong electron−electron interactions and Mott insulating state on the two-dimensional (2D) frustrated antiferromagnetic (AFM) checkerboard spin−lattice.[5−9] Very recently, bulk superconductivity was found in BiS_2-type layered compounds with mixed anions: $Bi_4O_4S_3$ and $Ln(O,F)BiS_2$.[10−12] Experimental and theoretical studies indicate that these materials exhibit multiband behaviors with dominant electron carriers originating from the Bi *6px* and *6px* bands in the normal state.[13−16] On the other hand, compounds with mixed anions exhibit remarkable flexibility of structure. Different two-dimensional (2D) building blocks, such as $[LnO]^+$, $[AEF]^+$ (AE = Ca, Sr, Ba), $[Ti_2OPn_2]^{2-}$, $[FePn]^-$, and $[TM_2OCh_2]^{2-}$, can sometimes be integrated to form new materials.[4,17−21] Individual building blocks often keep their structural and electronic properties after being combined together.[19]

In this work, we report the discovery of a new BiS_2-based layered compound, $SrFBiS_2$. It contains a NaCl-type BiS_2 layer and shows semiconducting behavior with relatively large thermopower. Theoretical calculations indicate that this compound is very similar to $LnOBiS_2$.

EXPERIMENT SECTION

Synthesis. $SrFBiS_2$ polycrystals were synthesized by a two-step solid-state reaction. First, Bi_2S_3 was prereacted by reacting Bi needles (purity 99.99%, Alfa Aesar) with sulfur flakes (purity 99.99%, Aldrich) in an evacuated quartz tube at 600°C for 10 h. Then Bi_2S_3 was mixed with stoichiometric SrF_2 (purity 99%, Alfa Aesar) and SrS (purity 99.9%, Alfa Aesar) and intimately ground together using an agate pestle and mortar. The ground powder was pressed into 10 mm diameter pellets. We used a maximum pressure of 5 tons. The pressed pellet was loaded in an alumina crucible and then sealed in quartz tubes with Ar under the pressure of 0.15 atm. The quartz tubes were heated to 600°C in 10 h and kept at 600°C for another 10 h.

Structure and Composition Analysis. Phase identity and purity were confirmed by powder X-ray diffraction carried out by a Rigaku Miniflex X-ray machine with Cu Kα radiation (λ = 1.5418 Å). Structural refinement of powder $SrFBiS_2$ sample was carried out by using Rietica software.[22] Synchrotron X-ray experiment was conducted at 300 K on a X17A beamline of the National Synchrotron Light Source (NSLS) at Brookhaven National Laboratory (BNL). The setup utilized a X-ray beam 0.5 mm × 0.5 mm in size and λ = 0.1839 Å (E = 67.4959 keV), conditioned by two-axis focusing with a one-bounce sagittally bent Laue crystal monochromator and Perkin-Elmer image plate detector mounted perpendicular to the primary beam path. A finely pulverized sample packed in a cylindrical polyimide capillary 1 mm in diameter was placed 204 mm away from the detector. Multiple scans were performed to a total exposure time of 120 s. The 2D diffraction data were integrated and converted to intensity versus 2θ using the software FIT2D.[23] The intensity data were corrected and normalized and converted to atomic pair distribution function (PDF), $G(r)$, using the program PDFgetX2.[24] The average stoichiometry of a $SrFBiS_2$ polycrystal was determined by examination of multiple points using an energy-dispersive X-ray spectroscopy (EDX) in a JEOL JSM-6500 scanning electron microscope.

Received: July 14, 2013
Published: August 29, 2013

Electrical and Thermal Transport Measurements. The sample pellets were cut into rectangular bars, and the surface is polished by sandpaper. Thin Pt wires were attached using silver epoxy for four probe resistivity measurements. Electrical and thermal transport measurements were carried out in quantum design physical property measurement system (PPMS-9).

Band Structure Calculations. First principle electronic structure calculations were performed using experimental crystallographic parameters within the full-potential linearized augmented plane wave (LAPW) method[25] implemented in the WIEN2k package.[26] The general gradient approximation (GGA) of Perdew et al.,[27] was used for exchange-correlation potential. The LAPW sphere radius were set to 2.5 Bohr for all atoms, and the converged basis corresponding to $R_{min}k_{max} = 7$ with additional local orbital were used, where R_{min} is the minimum LAPW sphere radius and k_{max} is the plane wave cutoff.

RESULTS AND DISCUSSION

Structure and Compostion. Figure 1(a) shows the powder XRD pattern of $SrFBiS_2$ measured by Rigaku Miniflex. Almost all of reflections can be indexed using the *P*4/*nmm* space group. The unidentified peaks belong to the second phase of Bi_2S_3. Using two-phase Le Bail fitting, the refined lattice parameters of $SrFBiS_2$ are a = 4.084(2) Å and c = 13.798(2) Å. When compared to $LaOBiS_2$, the a-axial lattice parameter is larger, and the c-axial one is slightly smaller.[11] The PDF structural analysis was carried out using the program PDFgui.[28] The $SrFBiS_2$ data are explained well within the model having *P*4/*nmm* symmetry with a = 4.079(2) Å and c = 13.814(5) Å (R_{wp} = 0.138, χ^2 = 0.024). It is consistent with the fitting results obtained from Miniflex. The final fit is shown in Figure 1(b), and the results are summarized in Table 1. In addition to the principal phase, the sample is found to have ~16(1) wt % of Bi_2S_3 impurity with *Pnma* symmetry, which is also observed in Figure 1(a). The structure of $SrFBiS_2$ is similar to $LaOBiS_2$, which is built up by stacking the rock salt-type BiS_2 layer and fluorite-type SrF layer alternatively along the c axis as shown Figure 1(c). The EDX spectrum of polycrystal confirms the presence of Sr, F, Bi, and S. The average atomic ratios determined from EDX are Sr:F:Bi:S = 1.00(4):1.00(9):1.03(5):1.88(4) when setting the content of Sr as 1. It confirms the formula of obtained compound is $SrFBiS_2$.

Electrical Properties. As shown in Figure 2, the resistivity $\rho(T)$ of $SrFBiS_2$ polycrystalline shows a semiconducting behavior in the measured temperature region (1.9−300 K). It should be noted that Bi_2S_3 polycrystal shows metallic behavior because of sulfur deficiency.[29] The impurity may have some minor influence on the absolute value of resistivity, but the semiconducting behavior should be intrinsic. Neglecting the grain boundary contribution, the room-temperature resistivity ρ(300 K) is about 0.5 Ω cm. Using the thermal activation model $\rho_{ab}(T) = \rho_0 \exp(E_a/k_BT)$ (ρ_0 is a prefactor, E_a thermal activated energy, and k_B the Boltzmann's constant) to fit the $\rho(T)$ at high temperature (75−300 K) (inset of Figure 2), we obtain E_a = 31.8(3) meV. The semiconductor behavior is consistent with theoretical calculation result shown below. On the other hand, theoretical calculations have indicated that undoped $LaOBiS_2$ is also a semiconductor, which is partially consistent with the experimental result.[13,30] The transport measurement indicates that $LaOBiS_2$ shows semiconducting behavior at T < 200 K but exhibit an upturn of resistivity at higher temperature. The origin of the upturn is unclear. Therefore, the replacement of LaO by SrF should not change the band structure and thus physical properties too much,

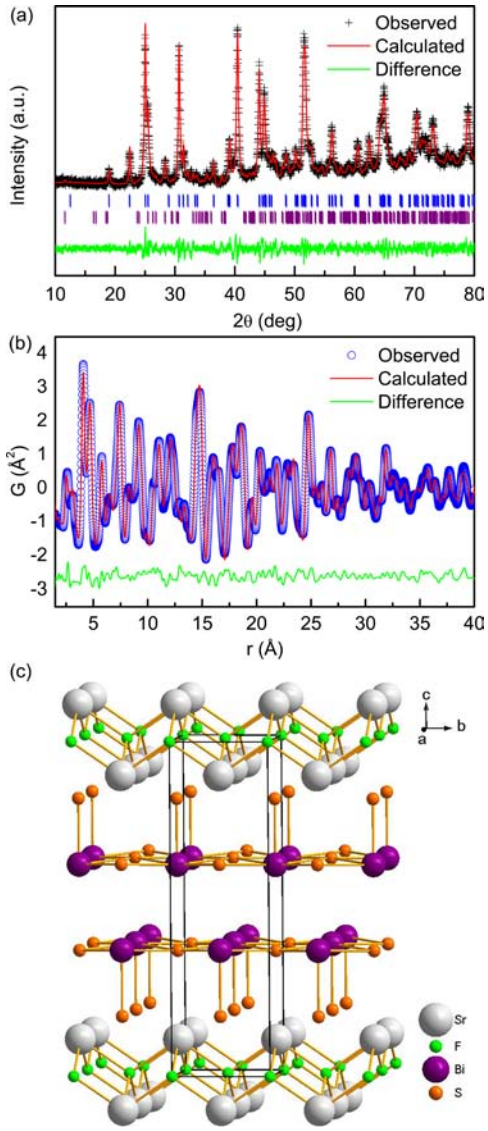

Figure 1. (a) Powder XRD pattern of $SrFBiS_2$ and the fitted result using two-phase Le Bail fitting. Crosses are experimental data. Red line is fitted spectra. Green line is the difference between experimental data and fitted spectra. Vertical lines are calculated Bragg positions for $SrFBiS_2$ (upper) and Bi_2S_3 (lower), respectively. (b) Synchrotron PDF refinement of data taken at room temperature. (c) Crystal structure of $SrFBiS_2$. The biggest white, big purple, medium orange, and small green balls represent Sr, Bi, S, and F ions, respectively.

especially at low temperature, similar to the relation between SrFFeAs and LaOFeAs.[18,31] The slight differences between $LaOBiS_2$ and $SrFBiS_2$, such as larger a-axial and smaller c-axial lattice parameters, could result in changing of physical properties at higher temperature. Note that the semiconducting $\rho(T)$ in $LaOBiS_2$ and $SrFBiS_2$ are different from those in parent compounds of iron pnictide superconductors. The latter show metallic behaviors at high temperature and a semiconducting-like upturn in the resistivity curve related to the spin density wave (SDW) transition. There is no significant magnetoresistance in $SrFBiS_2$ up to 90 kOe magnetic field.

Thermal Transport Properties. The temperature dependences of the thermal conductivity $\kappa(T)$ and thermoelectric power (TEP) $S(T)$ for $SrFBiS_2$ in zero field between 2 and 350 K are shown in Figure 3. The electronic thermal conductivity

dx.doi.org/10.1021/ic4018135 | Inorg. Chem. 2013, 52, 10685−10689

Table 1. Crystallographic Data for $SrFBiS_2$ Obtained from Synchrotron Powder XRD

chemical formula	$SrFBiS_2$
formula mass (g/mol)	379.73
crystal system	tetragonal
space group	$P4/nmm$ (No. 129)
a (Å)	4.079(2)
c (Å)	13.814(5)
V (Å^3)	229.8(3)
Z	2
density (g/cm^3)	5.51

atom	site	x	y	z	U_{eq} (Å^2)[a]
Sr	2c	1/4	1/4	0.1025(2)	0.0069(4)
F	2a	3/4	1/4	0	0.033(2)
Bi	2c	1/4	1/4	0.6286(5)	0.0183(3)
S1	2c	1/4	1/4	0.379(3)	0.060(2)
S2	2c	1/4	1/4	0.811(2)	0.019(1)

[a] U_{eq} is defined as one-third of the orthogonalized U_{ij} tensor.

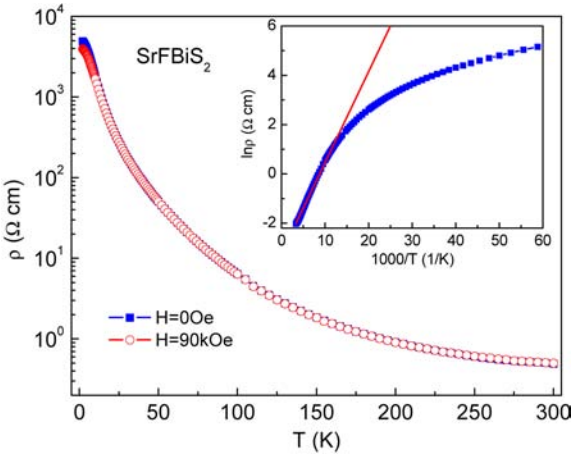

Figure 2. Temperature dependence of the resistivity $\rho(T)$ of the $SrFBiS_2$ at H = 0 (closed blue squares)and 90 kOe (open red circles). Inset shows the fitted result using thermal activation model for $\rho(T)$ at zero field, where the red line is the fitting curve.

$\kappa_e(T)$ estimated from the Wiedemann–Franz law using a value for the Lorenz number of 2.44×10^{-8} W Ω/K^2 was less than 5×10^{-6} of $\kappa(T)$. Therefore, lattice thermal conductivity dominates $\kappa_L(T)$, which exhibits a peak at around 60 K (Figure 1(a)). The peak in $\kappa(T)$ commonly arises because different phonon scattering processes usually dominate in different temperature ranges. Umklapp scattering dominates at high temperatures, while boundary and point-defect scattering dominate at low and intermediate temperatures, respectively.[32] On the other hand, the $\kappa(T)$ of $SrFBiS_2$ shows similar behavior to $Bi_4O_4S_3$ but with different peak position and absolute value.[16] For TEP $S(T)$ of $SrFBiS_2$, there is a reversal in sign at about 11 K, i.e, hole-like carrier changes into electron-like carrier, which is dominant at room temperature. According to two band model, $S = |S_h|\sigma_h - |S_e|\sigma_e/(\sigma_e + \sigma_h)$.[16] If we assume that S_h and S_e are temperature independent, it suggests that electron and hole conductivities change dramatically with temperature: at low temperature, $\sigma_h > \sigma_e$ whereas $\sigma_e > \sigma_h$ above 11 K. Hole-like carriers may originate from defect induced p-type doping. With increasing temperature, electron-like carriers due to intrinsic band excitation increase significantly, finally leading to $\sigma_e > \sigma_h$ and a sign change in $S(T)$. Similar behavior was observed in LaOZnP and p-type Si.[33,34] Even though the $S(T)$ in $SrFBiS_2$ is significant and not much smaller than in classics thermoelectric materials,[35] its low electrical conductivity makes its figure of merit ZT ($ZT = \sigma S^2 T/\kappa$) extremely small.

Electronic Structure. First principle calculations (Figure 4) confirm that $SrFBiS_2$ is a semiconductor with a direct band gap of 0.8 eV located at X point. This is similar to $LaOBiS_2$ where the energy gap was found to be 0.82 eV.[36] The calculation confirms the results of transport measurement. Similar to $LaOBiS_2$,[13,36] both S 3p and Bi 6p states are located around the Fermi level (−2.0 to 2.0 eV) in SrFBiS3p. Thus there is a strong hybridization between S 3p and Bi 6p states. The absence of dispersion along Γ–Z line suggests quasi two-dimensional character of the band structure in $SrFBiS_2$ (Figure 4(b)). In $LaOBiS_2$, F doping results in metallic states and superconductivity at low temperature. The main influence of F substitution is a carrier doping that shifts the Fermi level and has only a minor effect on the lowest conduction band. Because of the similarity between $SrFBiS_2$ and $LaOBiS_2$, new superconductors could be obtained by chemical substitution.

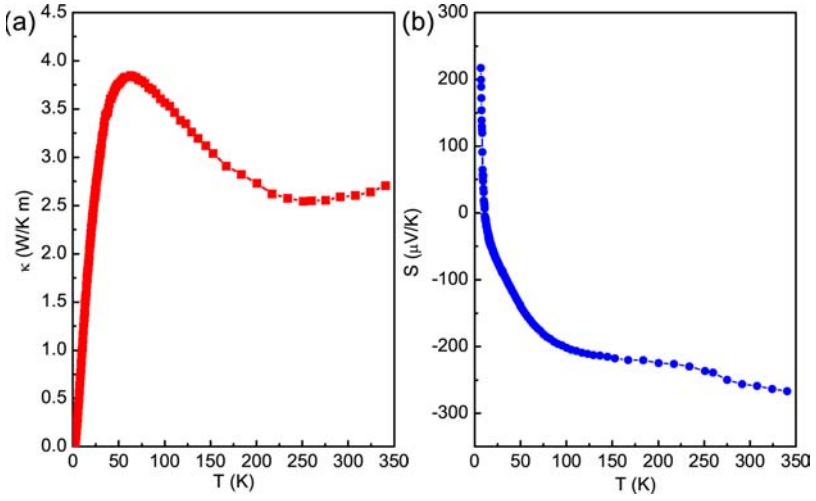

Figure 3. Temperature dependence of (a) thermal conductivity and (b) thermoelectric power for $SrFBiS_2$ under zero magnetic field within a temperature range from 2 to 340 K.

dx.doi.org/10.1021/ic4018135 | Inorg. Chem. 2013, 52, 10685–10689

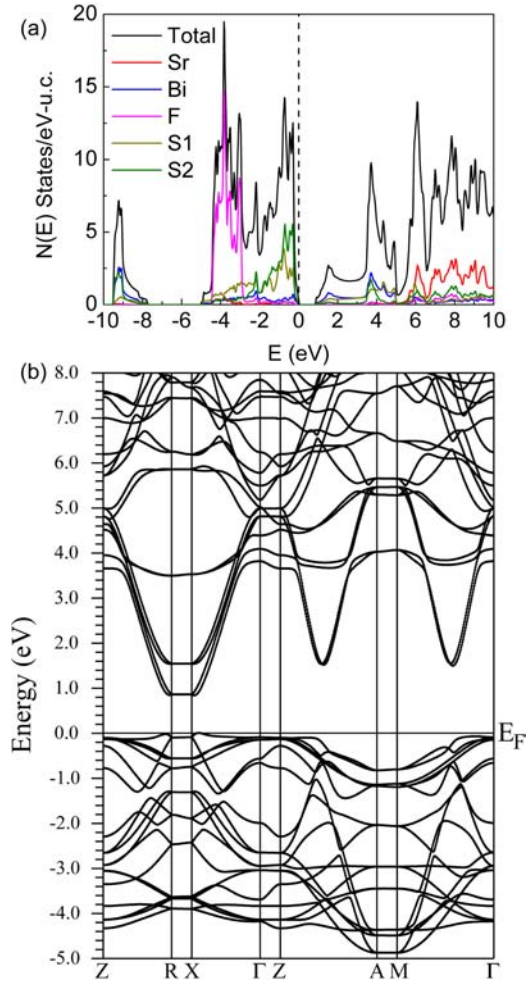

Figure 4. (a) Total and atom resolved density of states and (b) band structure of $SrFBiS_2$.

CONCLUSION

In summary, we report a discovery of a new layered fluorosulfide, $SrFBiS_2$. It contains a NaCl-type BiS_2 layer similar to $Bi_4O_4S_3$ and $Ln(O,F)BiS_2$ superconductors. $SrFBiS_2$ polycrystals show semiconducting behavior between 2 and 300 K. We observe rather small thermal conductivity and large TEP with sign reversal at low temperature. Theoretical calculation confirms the semiconducting behavior and indicates a similar DOS and band structure to undoped $LaOBiS_2$. Because of the similarity between $SrFBiS_2$ and the parent compound of BiS_2-based superconductors, it is of interest to investigate the doping effects on physical properties of $SrFBiS_2$. It could pave a way to new members in this emerging family of BiS_2-based superconductors.

ASSOCIATED CONTENT

Supporting Information

Data as mentioned in the text. This material is available free of charge via the Internet at http://pubs.acs.org.

AUTHOR INFORMATION

Corresponding Author

*E-mail: petrovic@bnl.gov.

Notes

The authors declare no competing financial interest.

ACKNOWLEDGMENTS

We thank John Warren for help with SEM measurements. Work at Brookhaven is supported by the U.S. DOE under Contract No. DE-AC02-98CH10886 and in part by the Center for Emergent Superconductivity, an Energy Frontier Research Center funded by the U.S. DOE, Office for Basic Energy Science (H.L. and C.P.). This work benefited from usage of X17A beamline of the National Synchrotron Light Source at Brookhaven National Laboratory. We gratefully acknowledge Zhong Zhong and Jonathan Hanson for their help with the X17A experiment setup.

REFERENCES

(1) Bednorz, J. G.; Muller, K. A. *Z. Physik B* **1986**, *64*, 189.
(2) Maeno, Y.; Hashimoto, H.; Yoshida, K.; Nishizaki, S.; Fujita, T.; Bednorz, J. G.; Lichtenberg, F. *Nature* **1994**, *372*, 532.
(3) Takada, K.; Sakurai, H.; Takayama-Muromachi, E.; Izumi, F.; Dilanian, R. A.; Sasaki, T. *Nature* **2003**, *422*, 53.
(4) Kamihara, Y.; Watanabe, T.; Hirano, M.; Hosono, H. *J. Am. Chem. Soc.* **2008**, *130*, 3296.
(5) Mayer, J. M.; Schneemeyer, L. F.; Siegrist, T.; Waszczak, J. V.; Van Dover, B. *Angew. Chem., Int. Ed. Engl.* **1992**, *31*, 1645.
(6) Wang, C.; Tan, M. Q.; Feng, C. M.; Ma, Z. F.; Jiang, S.; Xu, Z. A.; Cao, G. H.; Matsubayashi, K.; Uwatoko, Y. *J. Am. Chem. Soc.* **2010**, *132*, 7069.
(7) Zhu, J.-X.; Yu, R.; Wang, H.; Zhao, L. L.; Jones, M. D.; Dai, J.; Abrahams, E.; Morosan, E.; Fang, M.; Si, Q. *Phys. Rev. Lett.* **2010**, *104*, 216405.
(8) Ni, N.; Climent-Pascual, E.; Jia, S.; Huang, Q.; Cava, R. J. *Phys. Rev. B* **2010**, *82*, 214419.
(9) Free, D. G.; Withers, N. D.; Hickey, P. J.; Evans, J. O. *Chem. Mater.* **2011**, *23*, 1625.
(10) Mizuguchi, Y.; Fujihisa, H.; Gotoh, Y.; Suzuki, K.; Usui, H.; Kuroki, K.; Demura, S.; Takano, Y.; Izawa, H.; Miura, O. *Phys. Rev. B* **2012**, *86*, 220510(R).
(11) Mizuguchi, Y.; Demura, S.; Deguchi, K.; Takano, Y.; Fujihisa, H.; Gotoh, Y.; Izawa, H.; Miura, O. *J. Phys. Soc. Jpn.* **2012**, *81*, 114725.
(12) Demura, S.; Mizuguchi, Y.; Deguchi, K.; Okazaki, H.; Hara, H.; Watanabe, T.; Denholme, S. J.; Fujioka, M.; Ozaki, T.; Fujihisa, H.; Gotoh, Y.; Miura, O.; Yamaguchi, T.; Takeya, H.; Takano, Y. *J. Phys. Soc. Jpn.* **2013**, *82*, 033708.
(13) Usui, H.; Suzuki, K.; Kuroki, K. *Phys. Rev. B* **2012**, *86*, 220501(R).
(14) Li, S.; Yang, H.; Tao, J.; Ding, X.; Wen, H.-H. Multi-Band Exotic Superconductivity in the New Superconductor $Bi_4O_4S_3$. http://arxiv.org/abs/1207.4955.
(15) Singh, S. K.; Kumar, A.; Gahtori, B.; Shruti, G.; Sharma, S.; Patnaik; Awana, V. P. S. *J. Am. Chem. Soc.* **2012**, *134*, 16504.
(16) Tan, S. G.; Li, L. J.; Liu, Y.; Tong, P.; Zhao, B. C.; Lu, W. J.; Sun, Y. P. *Phys. C* **2012**, *483*, 94.
(17) Matsuishi, S.; Inoue, Y.; Nomura, T.; Yanagi, H.; Hirano, M.; Hosono, H. *J. Am. Chem. Soc.* **2008**, *130*, 14428.
(18) Han, F.; Zhu, X. Y.; Mu, G.; Cheng, P.; Wen, H.-H. *Phys. Rev. B* **2008**, *78*, 180503.
(19) Kabbour, H.; Cario, L.; Boucher, F. *J. Mater. Chem.* **2005**, *15*, 3525.
(20) Liu, R. H.; Zhang, J. S.; Cheng, P.; Luo, X. G.; Ying, J. J.; Yan, Y. J.; Zhang, M.; Wang, A. F.; Xiang, Z. J.; Ye, G. J.; Chen, X. H. *Phys. Rev. B* **2011**, *83*, 174450.
(21) Liu, R. H.; Song, Y. A.; Li, Q. J.; Ying, J. J.; Yan, Y. J.; He, Y.; Chen, X. H. *Chem. Mater.* **2010**, *22*, 1503.
(22) Hunter B. Rietica: A Visual Rietveld Program. International Union of Crystallography Commission on Powder Diffraction Newsletter No. 20, Summer, 1998. http://www.rietica.org.
(23) Hammersley, A. P.; Svenson, S. O.; Hanfland, M.; Hauserman, D. *High Pressure Res.* **1996**, *14*, 235.

(24) Qiu, X.; Thompson, J. W.; Billinge, S. J. L. *J. Appl. Crystallogr.* **2004**, *37*, 678.
(25) Weinert, M.; Wimmer, E.; Freeman, A. J. *Phys. Rev. B* **1982**, *26*, 4571.
(26) Blaha, P.; Schwarz, K.; Madsen, G. K. H.; Kvasnicka, D.; Luitz, J. *WIEN2k: An Augmented Plane Wave + Local Orbitals Program for Calculating Crystal Properties*; Technische Universitat Wien: Austria, 2001; ISBN: 3-9501031-1-2.
(27) Perdew, J. P.; Burke, K.; Ernzerhof, M. *Phys. Rev. Lett.* **1996**, *77*, 3865.
(28) Farrow, C. L.; Juhas, P.; Liu, J. W.; Bryndin, D.; Bozin, E. S.; Bloch, J.; Proffen, Th.; Billinge, S. J. L. *J. Phys.: Condens. Mater.* **2007**, *19*, 335219.
(29) Chen, B.; Uher, C.; Iordanidis, L.; Kanatzidis, M. G. *Chem. Mater.* **1997**, *9*, 1655.
(30) Awana, V. P. S.; Kumar, A.; Jha, R.; Kumar, S.; Kumar, J.; Pal, A. *Solid State Commun.* **2013**, *157*, 31−23.
(31) Dong, J.; Zhang, H. J.; Xu, G.; Li, Z.; Li, G.; Hu, W. Z.; Wu, D.; Chen, G. F.; Dai, X.; Luo, J. L.; Fang, Z.; Wang, N. L. *EPL* **2008**, *83*, 27006.
(32) Yang, J.; Morelli, D. T.; Meisner, G. P.; Chen, W.; Dyck, J. S.; Uher, C. *Phys. Rev. B* **2002**, *65*, 094115.
(33) Seeger, K. In *Semiconductor Physics: An Introduction*; Springer-Verlag, Berlin, 2004.
(34) Kayanuma, K.; Hiramatsu, H.; Hirano, M.; Kawamura, R.; Yanagi, H.; Kamiya, T.; Hosono, H. *Phys. Rev. B* **2007**, *76*, 195325.
(35) Rowe, D. M. In *Thermoelectrics Handbook: Macro to Nano*; Taylor & Francis: London, 2006.
(36) Wan, X.; Ding, H.-C.; Savrasov, S. Y.; Duan, C.-G. *Phys. Rev. B* **2013**, *87*, 115124.